Supplementary Information (SI) for Nanoscale.
This journal is © The Royal Society of Chemistry 2026

Supporting Information

Near-infrared photovoltaic gating enables polarity - reconfigurable WSe_2 phototransistors for in-sensor computing

Xueling Lu[†a,b], Yangyang Lv[†b], Haifeng Wu[†b], Jiali Yi[b], Guangcheng Wu[b], Huawei Liu[a*], Zhaoqian Wang[b], Qijun Zong[b], Qin Shuai[b], Lulu Huang[a], Huanghua Xu[b], Xinjian Li[c], Di Wu[c], Xiaoli Zhu[b*], Dong Li[b*] and Anlian Pan[a,b*]

[a]School of Physics and Electronics, Hunan Normal University, Changsha, Hunan, 410081, China

[b]Key Laboratory for Micro-Nano Physics and Technology of Hunan Province, State Key Laboratory of Chemo/Biosensing and Chemometrics, State Key Laboratory of Advanced Design and Manufacturing Technology for Vehicle, Hunan Institute of Optoelectronic Integration, College of Materials Science and Engineering, Hunan University, Changsha, 410082, China

[c]School of Physics and Microelectronics, Key Laboratory of Material Physics Ministry of Education, Zhengzhou University, Zhengzhou, Henan, 450052, China

[†]These authors contributed equally to this work.

*Email: hwliu@hnu.edu.cn, liidong@hnu.edu.cn, zhuxiaoli@hnu.edu.cn, anlian.pan@hnu.edu.cn

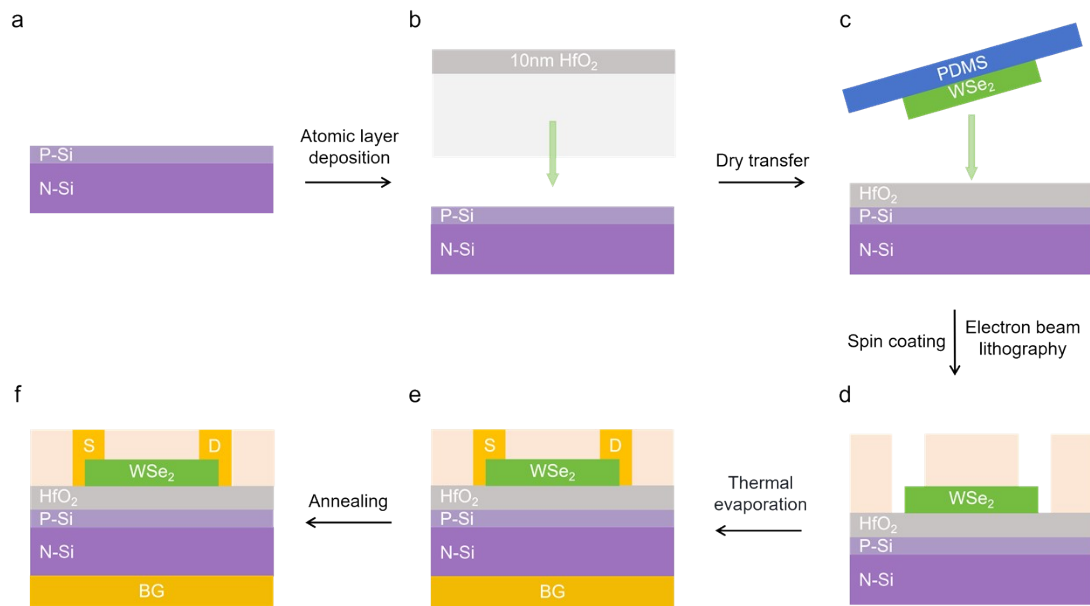

Figure S1. Schematic diagram of the device fabrication process. (a) Preparation of the Si PN junction substrate. (b) Deposition of a 10 nm-thick HfO_2 high-κ dielectric layer via atomic layer deposition (ALD). (c) Transfer of the mechanically exfoliated WSe_2 flake onto the substrate surface by a PDMS-assisted dry transfer technique. (d) Patterning of the source and drain electrodes via spin coating PMMA and electron beam lithography (EBL). (e) Deposition of metal contacts using thermal evaporation. (f) Schematic of the final device structure after thermal annealing to enhance contact quality.

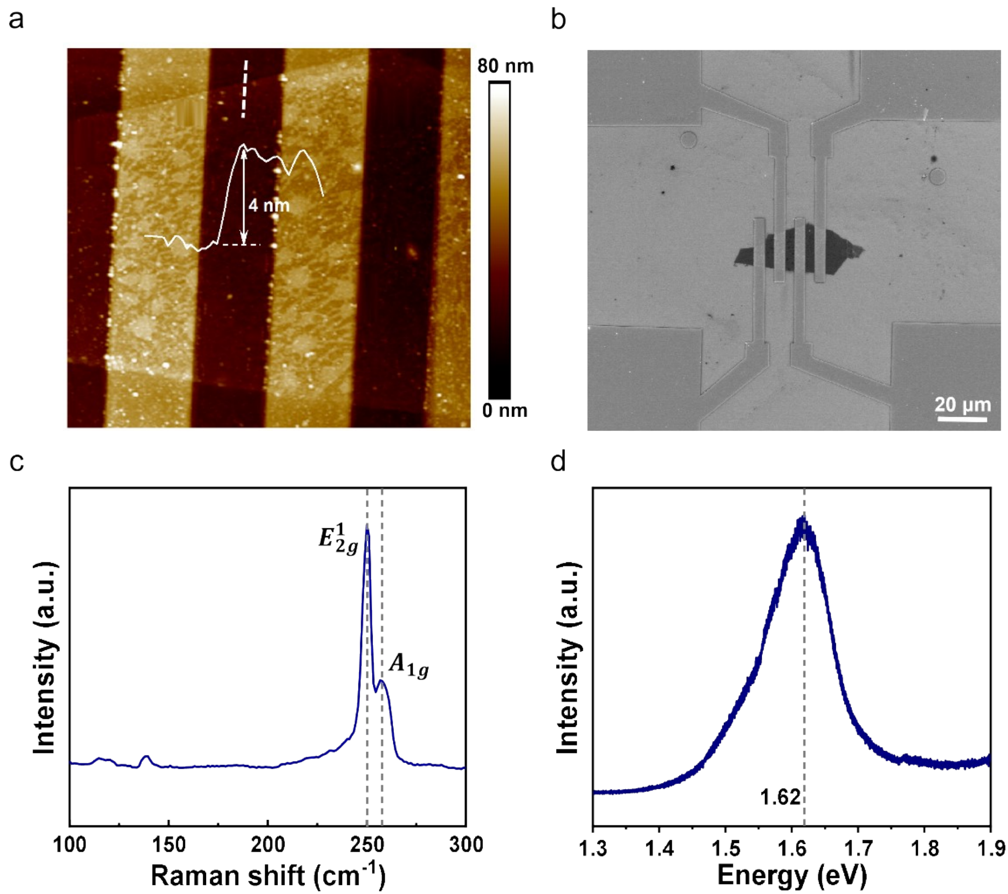

Figure S2. Device Characterization. (a) Atomic force microscopy (AFM) image of the sample and the thickness of the WSe_2 channel on the substrate. (b) SEM image of the samples, the scale bar is 20 μm. (c) Raman spectrum of the WSe_2 channel, the characteristic peaks confirm the high crystalline quality and few-layer nature. (d) Photoluminescence (PL) spectrum of WSe_2 under 532 nm laser excitation, displaying an emission typical of a few WSe_2 with a strong peak at 1.62 eV.

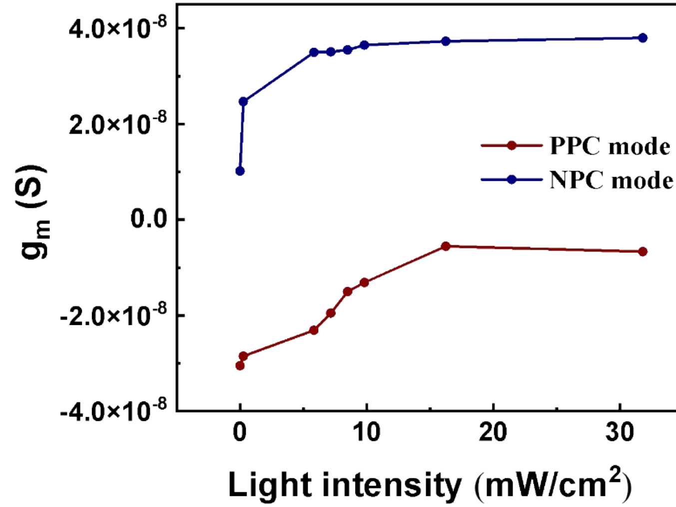

Figure S3. Transconductance (g_m) of the WSe_2 phototransistor as a function of light intensity under PPC-mode and NPC-mode operation. The transconductance is extracted from the transfer characteristics at a fixed drain bias. The results show that g_m increases with illumination intensity and exhibits distinct modulation behavior in the two operation modes, reflecting the tunable photogating effect induced by the Si PN junction.

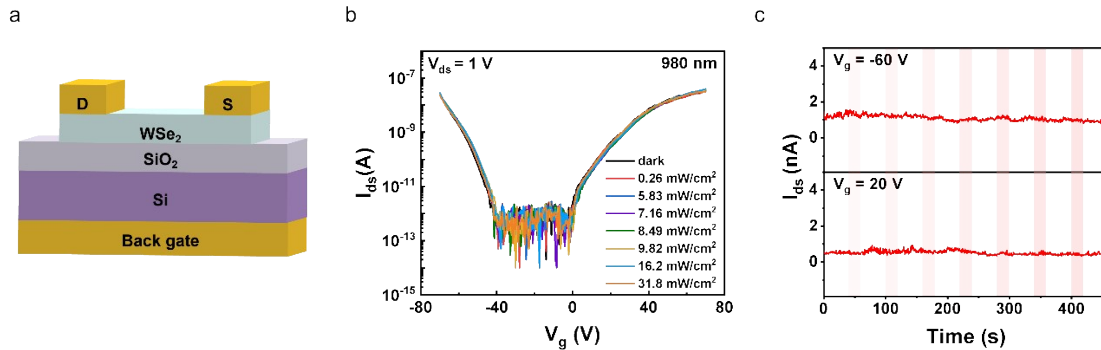

Figure S4. Control experiment performed on a $WSe_2/SiO_2/Si$ device. (a) Schematic diagram of the comparative device structure. (b) Transfer characteristic curves under 980 nm illumination with varying power densities. The overlapping curves exhibit no threshold voltage shift or photogating effect from the SiO_2/Si substrate, indicating the optical transparency of WSe_2 at this wavelength. (c) I-t curve measurements under fixed bias. The current remains at the baseline level without generating observable photocurrent during light switching. These results further effectively corroborating

that the photoresponse in the primary device originates exclusively from the photovoltaic effect of the underlying Si PN junction.

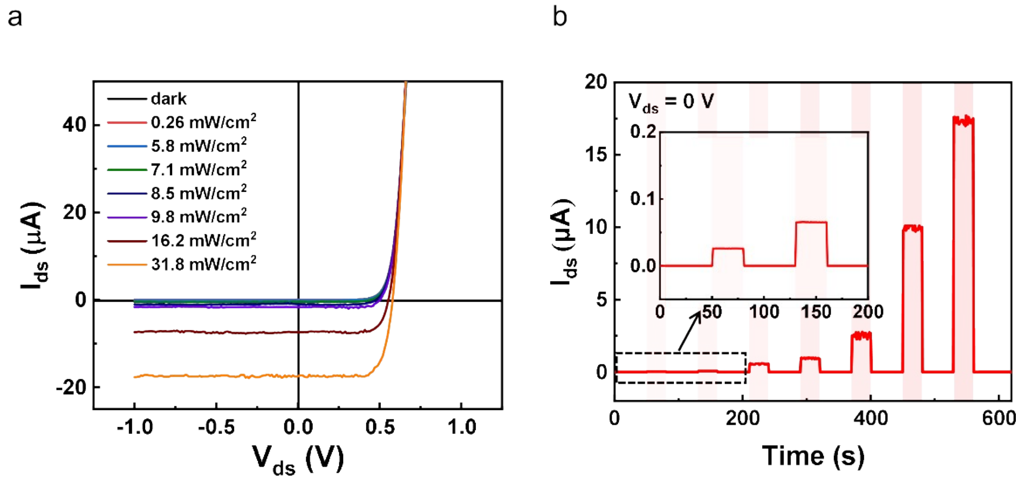

Figure S5. Control experiment characterizing the photovoltaic properties of the bare Si PN junction substrate (without WSe_2 channel). (a) I-V characteristic curves of the bare Si PN junction under varying light intensities at $V_g = 0$ V. The curves exhibit a distinct photovoltaic effect with a non-zero open-circuit voltage (V_{oc}) under illumination. This generated V_{oc} serves as the driving force for the threshold voltage shift observed in the device. (b) I-t photoresponse map at a fixed bias of $V_{ds} = 0$ V. The stepwise current modulation verifies the efficient generation of photocarriers and stable photovoltage by the substrate under infrared illumination, providing the photogating signal source for the overlying device.

Structure	wavelength (nm)	Mechanism	dark current (nA)	Responsivity (A/W)	Reconfigurable	Threshold voltage shift (V)	Ref.
WSe_2/HfO_2 /Si PN	980	Photovoltaic gating	~2/0.02	62.3/14.5	√	~0.4	This work
MoS_2/Si PN	780/880/970	Photovoltaic gating	400	~45	×	---	ACS Nano 2025, 19, 12053-12062
WSe_2/Ta_2NiSe_5 /SiO_2/Si	532/635/785	Photovoltaic	~10	~10^3	√	~0.4	ACS Nano 2025, 19, 1302-1315
WSe_2/hBN/MLG /SiO_2/Ge	532/1550	Photogating	~2/20	2.98	√	---	Adv. Sci. 2025, 12, e12649
WSe_2 homojunction /SiO_2/Si	405/670/808	Photogating	---	0.31	√	---	ACS Photonics 2026, 13, 1, 236-248
DPP-DTT/PDMS /Ag gate/PDMS	405/532/635 /808	Photoelectric	~9	~10	√	---	Nano Energy 2023, 110, 2211-2855

Table S1. Comparison of representative NIR phototransistors with reconfigurable capabilities reported in recent years. The table summarizes key device parameters, including structure, operating wavelength, operating mechanism, dark current, responsivity, detectivity, and reconfigurability[1-5].

Type	Wafer Orientation	Reference Agent	Resistance(Ω)	Thickness(μm)
P(Appearance)	(100)	B	3	1~2
N	(100)	SB	0.01-0.02	450

Table S2: Structural parameters of the Si PN junction substrate.

Material	Carrier type	Mobility	band gap	Electron affinity	Work function	Absorption range
WSe_2	Ambipolar	~10–200 $cm^2 V^{-1} s^{-1}$	1.62 eV	~3.9–4.0 eV	~4.5–5.0 eV	<765 nm

Table S3. Electrical and optical properties of WSe_2.

References:

1. S. S. Mousavi Khaleghi, J. Wei, Y. Liu, Y. Wang, Z. Fan, K. Li, J. Chen, R. Kudrawiec, R. Yang, K. B. Crozier and Y. Dan, *ACS Nano*, 2025, **19**, 12053-12062.
2. M. Liu, J. Wei, L. Qi, J. An, X. Liu, Y. Li, Z. Shi, D. Li, K. S. Novoselov, C.-W. Qiu and S. Li, *Nature Communications*, 2024, **15**, 141.
3. Q. Zhang, Y. Zhang, X. Liu, N. Zhang, T. Miao, H. Hu, L. Wang and Z. Zhu, *Advanced Science*, 2025, **12**, e12649.
4. X. Song, F. Liu, Z. Ma, X. Bie, H. Yang, Y. Jiang, S. Zhang, L. Yu, C. Jiang and C. Xia, *ACS Photonics*, 2026, **13**, 236-248.
5. S. Guo, H. Xu, Y. Zheng, L. Li, Z. Li, L. Zhang, H. Zhang, X. Wang, J. Li, L. Wang, L. Liu and Z. Lou, *Nano Energy*, 2023, **110**, 108361.